Available online at www.sciencedirect.com
ScienceDirect
C. R. Physique 8 (2007) 948–954
COMPTES RENDUS PHYSIQUE
http://france.elsevier.com/direct/COMREN/

Surfaces, interfaces, films

Origin and quantification of anomalous behaviour in velocity dispersion curves of stiffening layer/substrate configurations

Zahia Hadjoub [a], Imène Beldi [a,b], Abdellaziz Doghmane [a,*]

[a] *Laboratoire des semi-conducteurs, département de physique, faculté des sciences, Université Badji-Mokhtar, Annaba, BP 12, DZ-23000 Algeria*
[b] *Département des sciences fondamentales, faculté des sciences et sciences de l'ingénieur, Université 20.08.1955, Skikda, BP 26, DZ-21000 Algeria*

Received 20 November 2006; accepted after revision 9 August 2007

Available online 21 September 2007

Communicated by Jacques Villain

Abstract

Layer stiffening effects are studied via positive dispersion curves calculated for several layer/substrate configurations. The investigated layers (ZnO, Al, SiO_2, Cr, Si, SiC, AlN, Si_3N_4 and Al_2O_3) deposited on Cu and/or Si substrates, showed two types of anomalous behaviour: velocities greater than the layer Rayleigh velocity and those smaller that the substrate Rayleigh velocity. The appearance and disappearance of these phenomena are analysed and quantified in terms of a suggested elastic parameter, ξ, which shows that their origin is due the combined effect of the velocities and densities of both the layer and the substrate. ***To cite this article: Z. Hadjoub et al., C. R. Physique 8 (2007).***

Résumé

Origine et quantification des anomalies des courbes de dispersion des vitesses dans les structures films rigides/substrats. La détermination ainsi que la compréhension des phénomènes d'élasticité dans les couches minces sont indispensables pour la conception et la technologie de divers composants modernes. Dans ce contexte, l'effet de rigidité des films déposés sur des substrats est étudié via les courbes de dispersion positive ; ces courbes représentent la variation de la vitesse de propagation des ondes acoustiques en fonction de l'épaisseur des couches. La présente investigation de plusieurs combinaisons de films (ZnO, Al, SiO_2, Cr, Si, SiC, AlN, Si_3N_4 et Al_2O_3) déposés sur des substrats en Cu et/ou Si a révélé l'existence de deux types d'anomalies : (i) vitesse, V, plus élevée que celle de Rayleigh de la couche, V_{RL} ; et (ii) vitesse plus faible que celle de Rayleigh du substrat, V_{RS}. Ces phénomènes sont analysés et quantifiés en terme d'un paramètre élastique que nous avons défini comme étant le rapport des vitesses et des densités des films et des substrats. Ainsi, il nous a été possible de déduire que le premier cas, $V > V_{RL}$, apparaît pour $\xi < 0{,}4$; par contre le comportement inverse, $V < V_{RS}$, est obtenu pour $\xi > 1$. Les anomalies disparaissent pour $0{,}4 \leqslant \xi \leqslant 1$; dans cet intervalle on obtient les courbes de dispersion conventionnelles (augmentation initiale suivie d'une saturation). Par conséquent, ce comportement, quantifié avec succès par ξ, peut être attribué à l'effet combiné des vitesses et des densités. ***Pour citer cet article : Z. Hadjoub et al., C. R. Physique 8 (2007).***

Keywords: Thin films; Velocity dispersion; Reflection; Surface acoustic waves; Stiffening effect

* Corresponding author.
E-mail address: a_doghmane@yahoo.fr (A. Doghmane).

1631-0705/$ – see front matter
doi:10.1016/j.crhy.2007.08.001

Mots-clés : Couches minces ; Dispersion de la vitesse ; Réflexion ; Ondes acoustique de surface ; Effet de rigidité

1. Introduction

Numerical simulation of the different properties of bulk materials and thin films has become an indispensable tool for engineers who are involved in the design and technology of modern devices. However, to be able to accurately design structures and make exact predictions, in any field, it is necessary to know the mechanical properties of the materials that make up the structural components. Recent developments in this field indicate an increasing tendency to study the elastic properties of layers/substrate configurations, which play important roles in many technological, industrial and scientific fields. Among the most preferred micro-characterisation techniques are ultrasonic non-destructive methods which are generally based on the propagation of different modes in both bulk substrate and thin layers. The knowledge of the velocities of such vibrational modes can give a great wealth of information about the mechanical properties of the whole structure.

However, such velocities are characterized by what is the known dispersion behaviour, i.e. the dependence of the surface acoustic wave, SAW, velocity on the film thickness. The dispersive character of wave propagation is useful in evaluating material properties and density gradients with depth. According to SAW velocity values in layer/substrate structures, two opposite phenomena (loading and stiffening effects) appear. The layer is said to stiffen the substrate when its presence, at whatever thickness, increases the velocity of the surface wave above that of the Rayleigh velocity of the substrate and is said to load the substrate if it decreases the Rayleigh velocity [1–3]. Until recently, most reported investigations were carried out in the case of a 'slow on fast' combination characterised by negative dispersion curves (or mass loading effect), but little attention has been given to the case of a fast layer on a slow substrate exhibiting positive dispersion behaviour (or stiffness effect) [4–6]. The propagation of SAW on stiffening layers may show some anomalous behaviour [5–7] which was observed near cutoff, occurring when the velocity reaches the shear velocity of the substrate. However, the position of the cutoff point is not defined so clearly and the SAW propagation for the stiffening effect case is not yet fully understood since the interpretation was only based on velocity effects.

In this context, to enrich our comprehension, we analyse the stiffening effect by taking into account the densities of both layer and substrate, as well as their velocities, then determine a new combined acoustic parameter, ξ (incorporating velocities and densities of layer and substrate). Such a parameter is used to predict the origin, the appearance and disappearance of anomalous behaviour in velocity dispersion curves.

2. Calculation procedure

Ultrasonic investigations are based on surface acoustic waves which interact with the elastic properties of a given material into which different modes propagate. Among the most promising tools that have demonstrated a variety of unique capabilities in quantitative and qualitative characterisation of surface and subsurface details are scanning acoustic microscopes, SAM. The principles underlying the SAM have been described in detail elsewhere [8–10] and will not be reiterated here. Suffice to say that the simulation carried out in this study concerns the most conventional SAM under its normal operating conditions. Therefore, the obtained results can be directly verified experimentally using this instrument. The calculation procedure consists of several steps: (i) $V(z)$ calculation; (ii) $V(z)$ analysis and velocity determination; and (iii) velocity dispersion with layer thickness.

2.1. $V(z)$ calculation

The most important quantitative method for elastic parameters determination, in particular SAW velocities in scanning acoustic microscopy are acoustic material signatures, also known as $V(z)$, which are obtained by recording the output signal, V, as the distance, z, between the sample and the acoustic lens is varied. Such curves, that can be measured experimentally, can also be calculated theoretically, via the angular spectrum model [11], from the following expression:

$$V(z) = \int_0^{\pi/2} P^2(\theta) R(\theta) \left[\exp(2jk_0 z \cos\theta)\right] \sin\theta \cos\theta \, \mathrm{d}\theta \tag{1}$$

Here $P(\theta)$ is the pupil function, $k_0 = 2\pi/\lambda$ is the wave number in the coupling liquid, $j = \sqrt{-1}$, θ is the angle between the wave vector k and the lens axis and $R(\theta)$ is the reflectance function of the specimen. This last function, for acoustic waves, can be found by solving the acoustic Fresnel equation. The reflection coefficient [12–14] from a layer is:

$$R(\theta) = \frac{Z_{\text{in}} - Z_{\text{liq}}}{Z_{\text{in}} + Z_{\text{liq}}} \tag{2}$$

where Z_{liq} is the impedance of plane wave in the liquid, Z_{in} is the input impedance of the layer, that is, the impedance at the boundary: layer–liquid, which is expressed by the formula:

$$Z_{\text{in}} = Z_{\text{L}} \frac{Z_{\text{s}} - \text{i}Z_{\text{L}} \tan\varphi}{Z_{\text{L}} - \text{i}Z_{\text{s}} \tan\varphi} \tag{3}$$

with $\varphi = k_{\text{L}} h \cos\theta_{\text{L}}$ being the phase advance of the plane wave passing through the layer of an h thickness and Z_{s} and Z_{L} are the acoustic impedances of substrate and layer, respectively, given by:

$$Z|_{i=\text{liq,L,s}} = \frac{\rho_i V_i}{\cos\theta_i} \tag{4}$$

where subscripts liq. L and s stand for liquid, layer and substrate, respectively. It is clear that at normal incidence the acoustic impedance becomes simply the product of density and velocity. Hence, the intensity reflection coefficient of a layer on a substrate is:

$$R = \frac{Z_{\text{L}}^2 (Z_{\text{s}} - Z_{\text{liq}})^2 \cos^2 k_{\text{L}} h + (Z_{\text{s}} Z_{\text{liq}} - Z_{\text{L}}^2)^2 \sin^2 k_{\text{L}} h}{Z_{\text{L}}^2 (Z_{\text{s}} + Z_{\text{liq}})^2 \cos^2 k_{\text{L}} h + (Z_{\text{s}} Z_{\text{liq}} + Z_{\text{L}}^2)^2 \sin^2 k_{\text{L}} h} \tag{5}$$

Note that the reflection coefficient is a complex-valued function with an amplitude and a phase and the total reflection is obtained for $|R(\theta)| = 1$. Therefore, the $V(z)$ calculation from relation (1) can readily be carried out by just knowing the SAW velocities and material densities.

2.2. *Velocity dispersion determination*

The schematic representation of $V(z)$ curves, given by Eq. (1), is shown in Fig. 1(a); it consists of many peaks and valleys due to constructive and destructive interference between different propagating modes, with a main peak

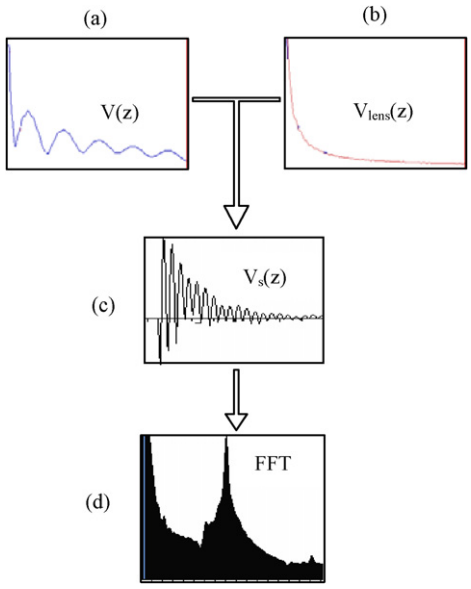

Fig. 1. Schematic diagram showing different calculation steps: (a) $V(z)$ signature, (b) lens response, (c) sample signature and (d) FFT spectrum.

at the focal distance ($z = 0$) representing the lens response. However, successive peaks decay exponentially when z increases, as a result of the influence of the acoustic lens signal, V_{lens} (Fig. 1(b)). Thus, the real signal of the specimen, $V_s(z)$, would be: $V(z) - V_{\text{lens}}(z)$.

The signal, thus obtained (Fig. 1(c)), is a periodic curve characterised by a spatial period Δz. Hence, its treatment can be carried out via fast Fourier transform, FFT, which exhibits a large spectrum consisting of one or several peaks (Fig. 1(d)). The dominant mode (usually Rayleigh) appears as a very sharp and pronounced peak from which the Rayleigh velocity can be determined [15,16] according to the relation:

$$V_R = \frac{V_{\text{liq}}}{\sqrt{1 - (\frac{V_{\text{liq}}}{2f\Delta z})^2}} \tag{6}$$

where V_{liq} is the sound velocity in the coupling liquid and f the operating frequency.

The final main step consists of (i) determining Rayleigh velocity for each layer/substrate structure for variable layer thickness as described above and (ii) plotting V_R as a function of normalised thickness, h/λ_L, where λ_L is the wavelength of the transverse waves propagating in the layer. The calculation was performed in the range $0 < h/\lambda_L < 2$; the lower value ($h = 0$) represents a naked substrate without a layer whereas the highest value ($h = 2\lambda_L$) describe the case when the layer become so thick to be considered as a bulk material. The aforementioned steps were repeated for several layers/substrates combinations.

3. Materials and simulation conditions

Several layers (ZnO, Al, SiO_2, Cr, Si, SiC, AlN, Si_3N_4 and Al_2O_3) deposited on either Cu or Si substrates were considered. Their elastic parameters [17] are summarised in Table 1, which lists the densities and longitudinal, transverse and Rayleigh velocities. These materials were chosen such that they illustrate two types of combinations, one when the properties of the layer and the substrate are close and the other when they are dissimilar. Table 2 regroups relative velocities (first line) and densities (second line) of layers and substrates.

Calculations were carried out in the case of a conventional scanning acoustic microscope working in the reflection mode at an operating frequency of 142 MHz, with a half-opening angle of 50° and water as a coupling liquid. It is well

Table 1
Elastic properties of investigated real materials and fictitious materials Mx_i

	Materials	ρ (kg/m)	V_L (m/s)	V_T (m/s)	V_R (m/s)
Layers	ZnO	5606	6400	2950	2765
	Al	2698	6300	3080	2880
	SiO_2	2600	5980	3700	3397
	Cr	7194	6608	4005	3661
	SiC	3210	12 099	7485	6806
	AlN	3260	10 012	7647	6418
	Si_3N_4	3185	10 607	6204	5694
	Al_2O_3	3980	11 150	6036	5600
	Mx_1	7194	6400	2950	2765
	Mx_2	2300	6300	3080	2880
	Mx_3	2600	11 150	6036	5600
	Mx_4	7194	12 099	7485	6806
Substrates	Si	2300	9160	5085	4712
	Cu	8900	4700	2260	2118

Table 2
Relative elastic properties (velocities and densities) of different films/substrate structures used in this investigation where $\xi = (\rho_L/\rho_S)/(V_{RL}/V_{RS})$

Structure	$\frac{SiC}{Cu}$	$\frac{AlN}{Cu}$	$\frac{Si}{Cu}$	$\frac{Si_3N_4}{Cu}$	$\frac{SiO_2}{Cu}$	$\frac{Al}{Cu}$	$\frac{Cr}{Cu}$	$\frac{ZnO}{Cu}$	$\frac{SiC}{Si}$	$\frac{AlN}{Si}$	$\frac{Si_3N_4}{Si}$	$\frac{Al_2O_3}{Si}$	$\frac{Mx_1}{Cu}$	$\frac{Mx_2}{Cu}$	$\frac{Mx_3}{Si}$	$\frac{Mx_4}{Si}$
V_{RL}/V_{RS}	3.23	3.03	2.22	2.69	1.60	1.37	1.73	1.31	1.45	1.36	1.21	1.19	1.36	1.33	1.19	1.45
ρ_L/ρ_S	0.36	0.37	0.26	0.36	0.29	0.30	0.81	0.63	1.40	1.42	1.38	1.73	0.81	0.26	1.13	3.13
ξ	0.11	0.12	0.12	0.13	0.18	0.22	0.47	0.48	0.96	1.04	1.14	1.45	0.60	0.20	0.95	2.16

established that under these normal operating conditions V_R can easily be deduced since the most dominant mode is that of Rayleigh.

4. Results and discussions

4.1. Anomalous behaviour observation

To show the effect of layer thickness on V_R, we plot in Fig. 2(a) and 2(b) typical curves of some of the investigated layers deposited on Cu and Si substrates, respectively. Conventionally, the velocity increases initially from that of the substrate, V_{RS}, then saturates when it approaches asymptotically a value that corresponds to the Rayleigh velocity of each layer, V_{RL}. However, in the present case, these variations are not obtainable for all layer/substrate combinations; some anomalies are obtained.

In region II ($0.2 < h/\lambda_L < 1$) of Fig. 2(a), which is enlarged in Fig. 3(a), one can clearly notice the appearance of an anomalous behaviour (*velocities higher than those of the layer Rayleigh velocity*, V_{RL}). In fact, after the usual initial increase in velocity in region I ($0 < h/\lambda_L < 0.2$), we observe a very sharp increase leading to a peak which

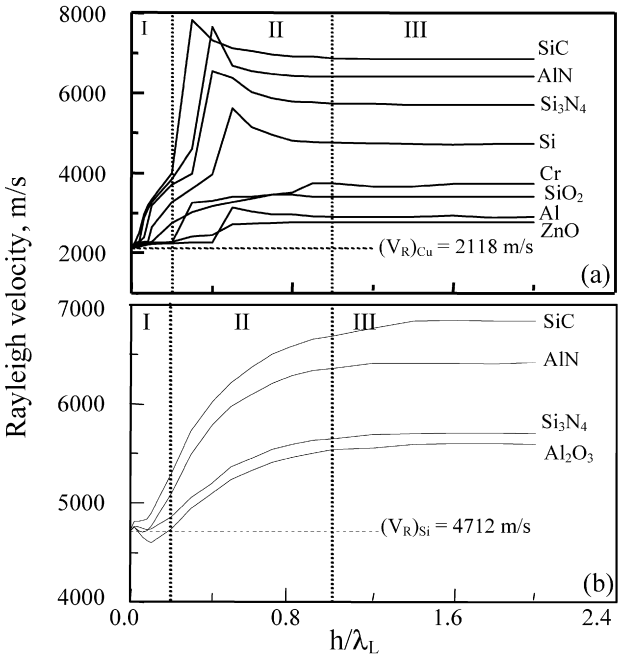

Fig. 2. Velocity dispersion curves for several layer/Cu structures (a) and layer/Si structures (b).

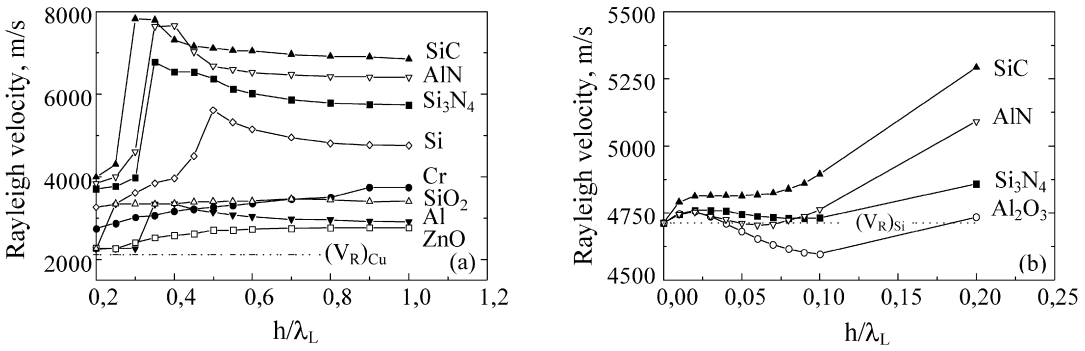

Fig. 3. Anomalous behaviors in velocity dispersion curves for region II in layer/Cu structures (a) and region I in layer/Si structures (b).

overtakes 'abnormally' the layer Rayleigh velocity. The highest and the sharpest peak was obtained for the SiC layer, whereas, for other layers (AlN, Si_3N_4, Si, Cr, SiO_2, Al and ZnO), such a peak seems to show (i) a decrease in height, (ii) a broadening, (iii) a shift towards greater normalized thickness and (iv) even a complete disappearance.

In region I of Fig. 2(b), which is enlarged in Fig. 3(b), one can observe for layers/Si configurations the appearance of an inverse anomalous behaviour (*velocities lower than those of the substrate Rayleigh velocity*, V_{RS}). Such behaviour differs in both shape and amplitude according to layer and substrate properties, i.e. velocities and densities. It should be noted that a similar behaviour was experimentally observed [18] for diamond-like-carbon layers on silicon substrates, investigated at 200 and 600 MHz by line- and point-focus beam acoustic microscopes.

4.2. Quantification

In order to analyse these unusual phenomena, we considered the influence of different parameters by associating the effect of velocities and densities; this procedure would lead to the appearance or disappearance of anomalous behaviour in velocity dispersion curves. In this context, we first considered Al/Cu and Al_2O_3/Si structures which presented strong anomalous behaviour and ZnO/Cu and SiC/Si combinations which showed a normal evolution of dispersion curves (Fig. 2(a) and (b)). Then, we introduced, four fictitious materials Mx_1, Mx_2, Mx_3 and Mx_4 whose longitudinal and transverse velocities are similar to those of Al, ZnO, Al_2O_3 and SiC, respectively, whereas their densities are either too high or too low (last four rows in Table 2). The deduced velocity dispersion curves (- - -) for the structures Mx_1/Cu, Mx_2/Cu, Mx_3/Si and Mx_4/Si are illustrated in Fig. 4; we also included, for comparison, real structures (——): Al/Cu, ZnO/Cu, Al_2O_3/Si and SiC/Si. It can clearly be seen that both types of the anomalous behaviour observed with real layers (——), in Figs. 4(a) and (c), disappeared for fictitious materials (- - -), whereas, it was possible (Figs. 4(b) and (d)) to create both types of anomalous behaviour with fictitious films (- - -) which were absent in real structures (——).

To quantify the existence of these anomalous phenomena, we introduce a new elastic parameter, ξ, which takes into account densities and velocities of both substrates and layers; it is defined as $\xi = (\rho_L/\rho_S)/(V_{RL}/V_{RS})$. In the present work, the values of this parameter were varied, from 0.11 to 2.16 (Table 2). From a close analysis of the influence of ξ values on the appearance or disappearance of the anomalous behaviour, in dispersion curves, it can be concluded that:

(i) the unexpected phenomenon (*velocity greater than the layer* V_{RL}), in Figs. 2(a) and 3(a), occurs for $\xi < 0.4$. Such behaviour gets more enhanced when ξ values become smaller, as in the cases of SiC/Cu and AlN/Cu whose

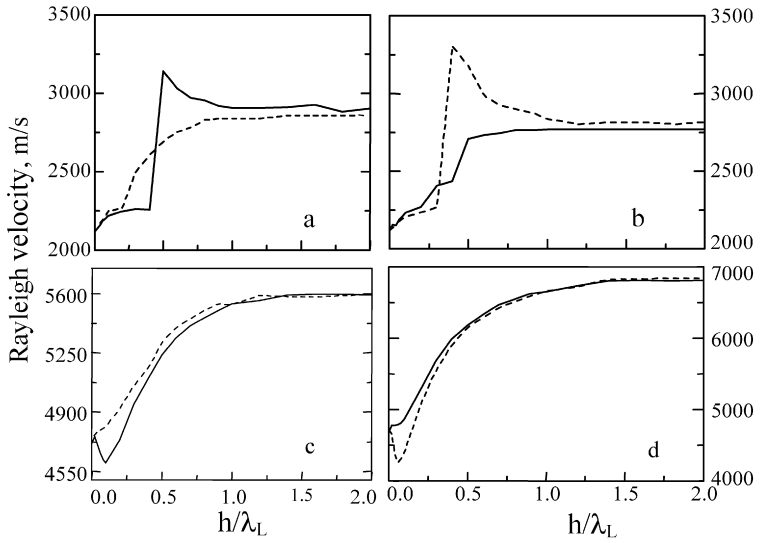

Fig. 4. Velocity dispersion curves for real (——) and fictitious materials, Mx_i (- - -): (a) Al/Cu and Mx_1/Cu; (b) ZnO/Cu and Mx_2/Cu; (c) Al_2O_3/Si and Mx_3/Si; (d) SiC/Si and Mx_4/Si.

ξ are 0.11 and 0.12, respectively. This deduction is further confirmed when considering $\xi = 0.2$ for Mx_2/Cu in Fig. 4(b) which led the appearance of such a behaviour.

(ii) the inverse anomalous behaviour (*velocity smaller than the substrate* V_{RS}), in Figs. 2(b) and 3(b), dominates for $\xi > 1$. This behaviour becomes more enhanced for structures characterised by higher values of ξ as in the cases of Si_3N_4/Si and Al_2O_3/Si whose ξ are 1.14 and 1.45, respectively. Such a behaviour is also obtained by the choice of $\xi = 2.16$ for Mx_4/Si (Fig. 4(d)); thus confirming the observations with real structures.

(iii) the anomalous behaviour disappears for $0.4 \leqslant \xi \leqslant 1$ as illustrated by ZnO/Cu and SiC/Si combinations whose ξ are 0.48 and 0.96, respectively. The choice of $\xi = 0.6$ for Mx_1/Cu (Fig. 4(a)) and $\xi = 0.95$ for Mx_3/Si (Fig. 4(c)) supports this conclusion because, in both cases, no anomalous behaviour was obtained.

Therefore, it is safe to conclude that both velocity and density of stiffening layers and substrates, expressed by their combined parameter ξ, play an important role in the appearance and disappearance of anomalous behaviour. The importance of such investigation lies in the possibility of predicting and distinguishing several types of dispersion behaviour depending on the relative properties of the layer and substrate by just knowing the elastic parameter ξ. It also enriches and completes the understanding of surface wave propagation for the characterisation of hard materials [5,6], the investigation of this behaviour at certain limits which were explained in terms of relative shear velocities [1,2] as well as the interpretation of the acoustoelastic anomaly in stressed heterostructures [19].

5. Conclusion

Anomalous behaviour, obtained in velocity dispersion curves of stiffening layers, was shown to be influenced by not only the velocity but also the density of both layer and substrate. Introducing a new elastic parameter $\xi = (\rho_L/\rho_S)/(V_{RL}/V_{RS})$ enabled us to conclude that the unexpected phenomenon (velocity greater than the layer V_R) occurs for $\xi < 0.4$; whereas, the inverse anomalous behaviour (velocity smaller than the substrate V_R), dominates for $\xi > 1$. However, for $0.4 \leqslant \xi \leqslant 1$ the anomalous behaviour disappears completely leading to conventional variations of velocity dispersion curves. Thus, this investigation has shown that the combined effect of velocity and density is at the origin of the existence of unexpected behaviour in positive velocity dispersion curves.

References

[1] G.W. Farnell, E.L. Adler, in: R.N. Thurson, P.W. Mason (Eds.), Physical Acoustics, vol. X, Academic Press, New York, 1972, pp. 35–127.
[2] G.W. Farnell, in: A.A. Oliner (Ed.), Acoustic Surface Waves, Springer-Verlag, Berlin, 1978, pp. 13–60.
[3] W.-S. Ohm, M.F. Hamilton, J. Acoust. Soc. Am. 115 (2004) 2798.
[4] Z. Hadjoub, I. Beldi, M. Bouloudenine, A. Gacem, A. Doghmane, Electron. Lett. 34 (1998) 313.
[5] O. Lefeuvre, P. Zinin, G.A.D. Briggs, A. Every, Appl. Phys. Lett. 72 (1998) 856.
[6] P. Zinin, O. Lefeuvre, G.A.D. Briggs, B.D. Zeller, P. Cawley, A.J. Kinloch, G.E. Thompson, J. Appl. Phys. 82 (1997) 1031.
[7] R.D. Weglein, G. Kim, Ultrasonics Symp. (1981) 727.
[8] A. Briggs (Ed.), Advances in Acoustic Microscopy, Plenum Press, New York, 1995.
[9] Z. Yu, S. Boseck, Rev. Mod. Phys. 67 (1995) 863.
[10] S. Bouhedja, I. Hadjoub, A. Doghmane, Z. Hadjoub, Phys. Stat. Sol. (a) 202 (2005) 1025.
[11] C.G.R. Sheppard, T. Wilson, Appl. Phys. Lett. 38 (1981) 858.
[12] L.M. Brekhovskikh, Wave in Layered Media, Academic Press, New York, 1980.
[13] L.M. Breekhovskikh, O.A. Godin, Acoustics of Layered Media I, Springer-Verlag, Berlin, 1990.
[14] I. Beldi, Z. Hadjoub, A. Doghmane, Phys. Chem. News (2007), in press.
[15] J. Kushibiki, N. Chubachi, IEEE Sonics Ultrason. SU-32 (1985) 189.
[16] Y. Ohashi, J. Kushibiki, IEEE Trans. Ultrasonics Ferroelectr. Freq. Control 51 (2004) 686.
[17] A. Briggs, Acoustic Microscopy, Clarendon Press, Oxford, 1992.
[18] R.D. Weglein, J.O. Kim, Ultrasonics Symp. (1991) 727.
[19] E. Chilla, A.V. Osetrov, R. Kokh, Phys. Rev. B 63 (2001) 113308.